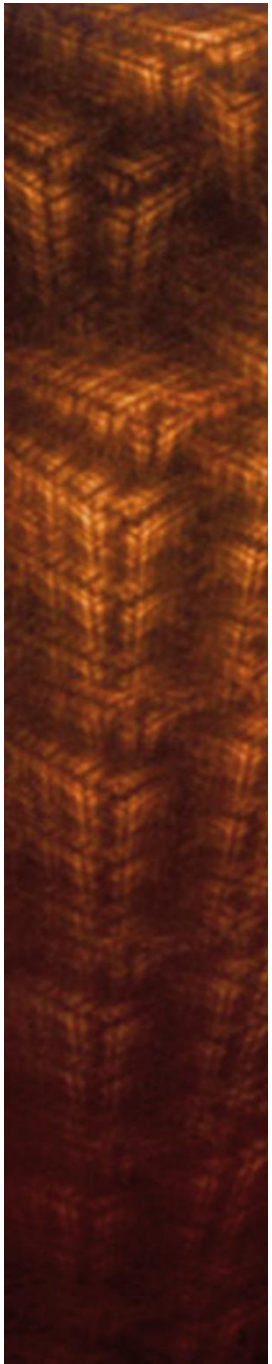

institute imdea materials

EUROPEAN UNION
STRUCTURAL FUNDS

La Suma de Todos
Comunidad de Madrid
www.madrid.org

8th International Conference on Composites testing and Model Identification (COMPTEST2017), Leuven 5th April 2017

Microscale testing techniques for constituent characterization in computational micromechanics

F. Naya, M. Monclús, J. Molina-Aldareguía, C.González, C.S. Lopes

AIRBUS

Composite Materials Group

Motivation

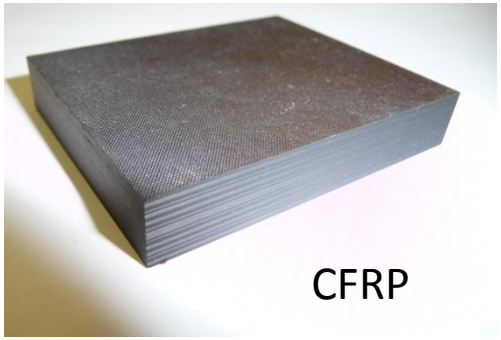

CFRP

MATERIAL CERTIFICATION (2 years)

Predicting mechanical properties and failure mechanisms under different environmental conditions → **Extensive and costly experimental program**

Bottom-up multiscale simulation strategy [1]

To reduce time and cost associated to composite testing by means of computational micromechanics from the properties of the constituents

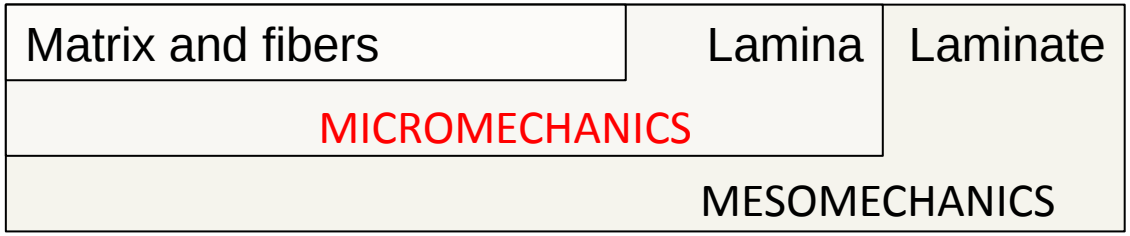

[1] Llorca J., González C., Molina-Aldareguía J.M., et al, 2011 . Multiscale modeling of composite materials: a roadmap towards virtual testing. Adv. Mater. 23,5130–5147.

Bottom-up multiscale

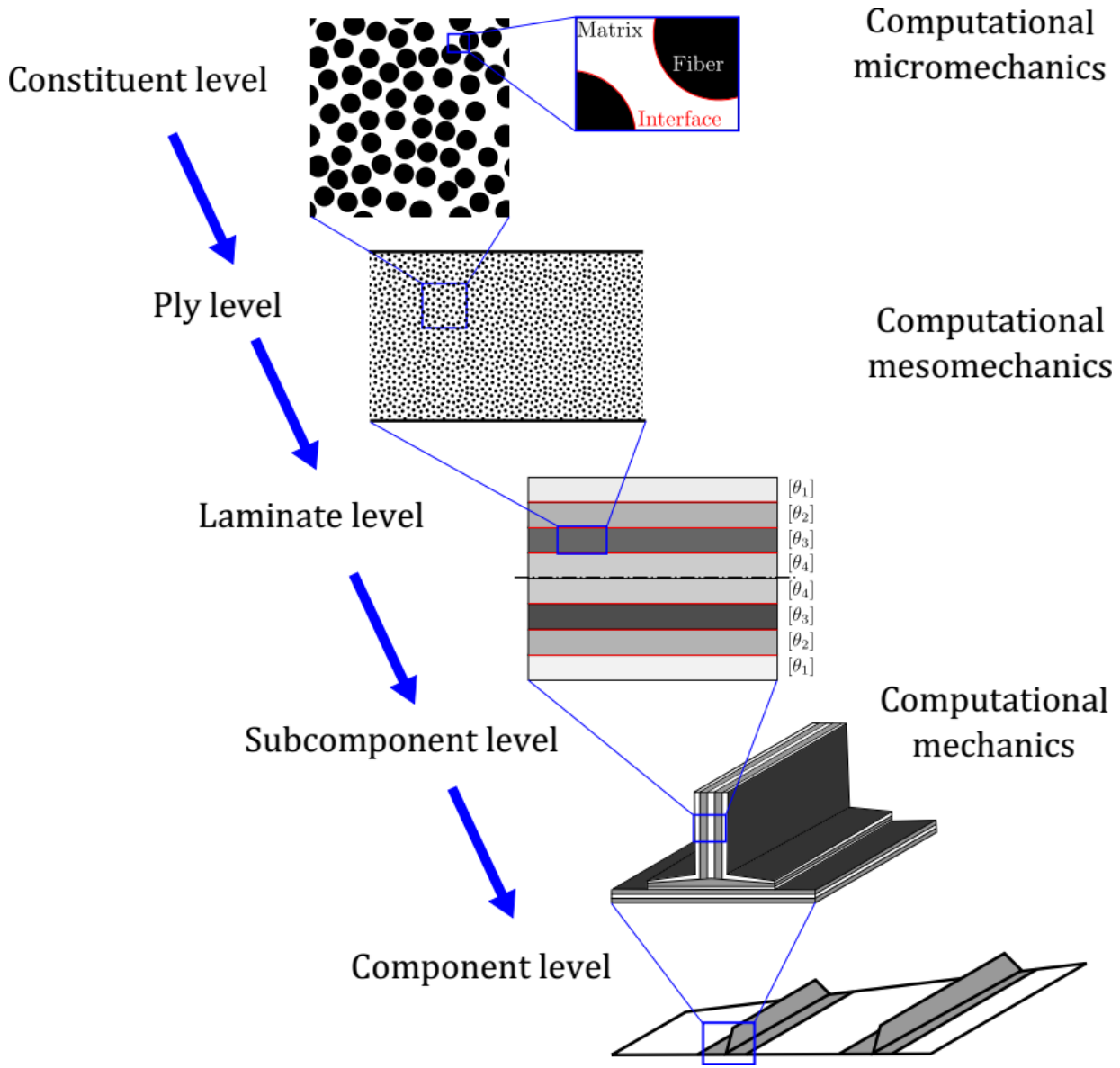

Bottom-up multiscale

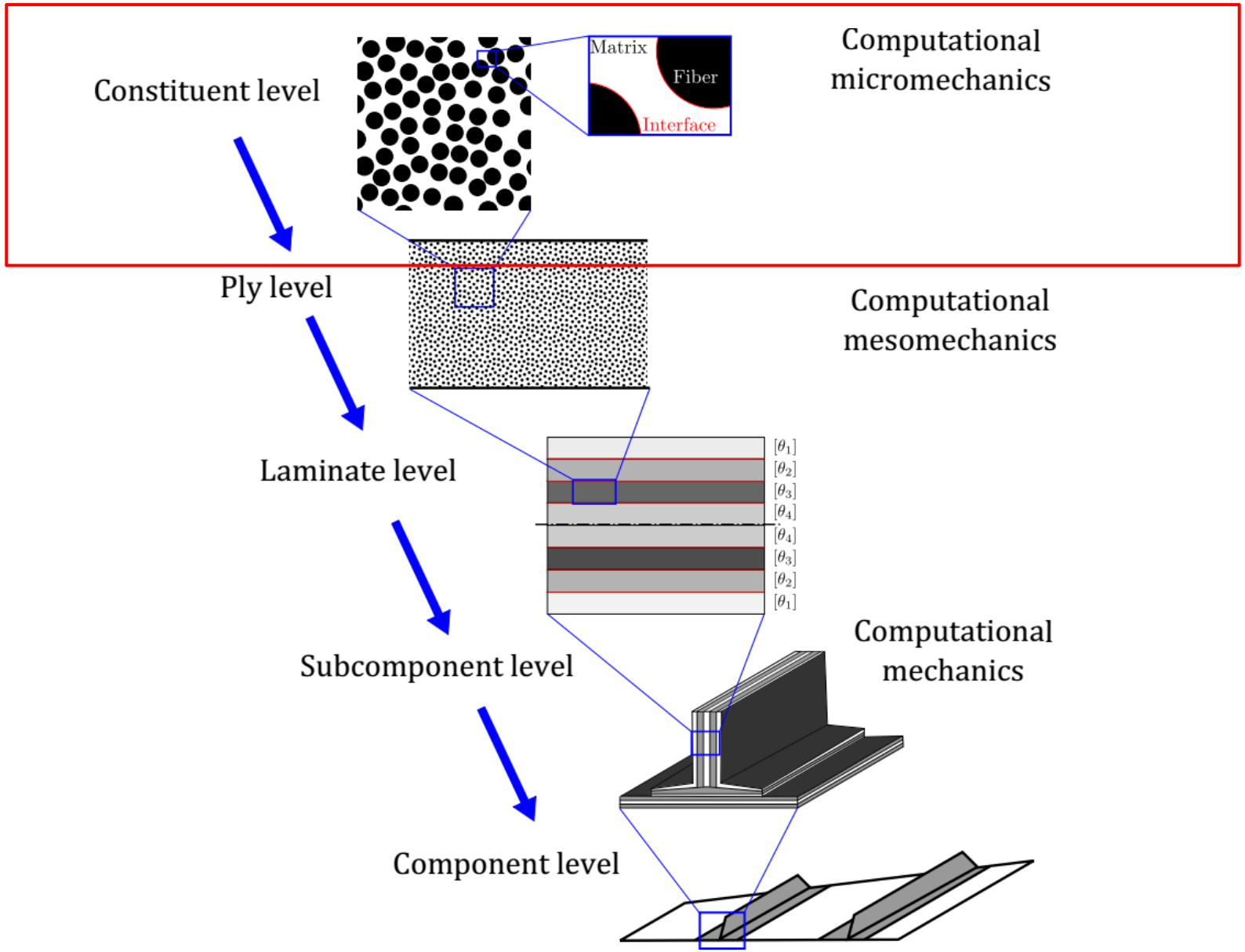

Objectives

Experimental micromechanics

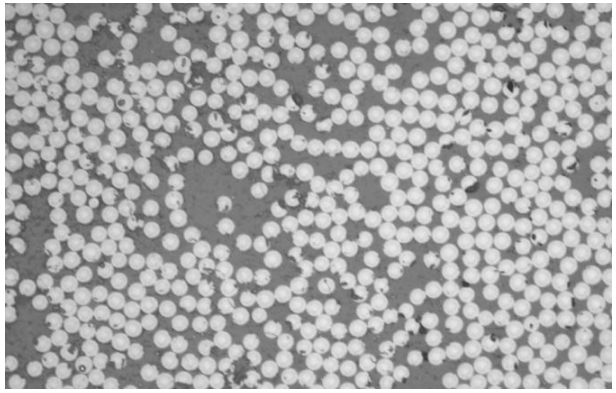

Composite UD ply

Computational micromechanics

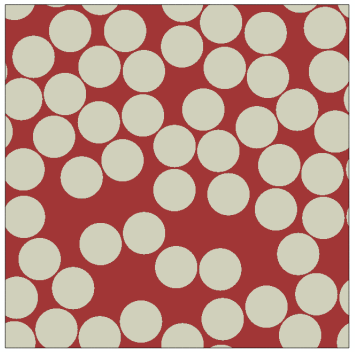

Periodic RVE

Homogenization

Ply behavior

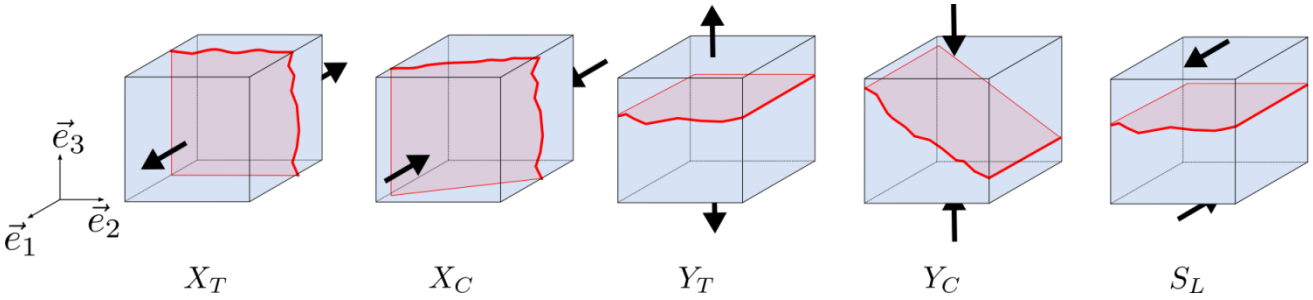

Material

AS4/8552:

- Carbon Fiber Reinforced Polymer (V_f = 58%)
- Provided by the customer (Airbus)
- UD stacking sequence is $[0]_{12}$
- Autoclave cured (2h T=130 C + 2h T=180 C at 6.2 bar)

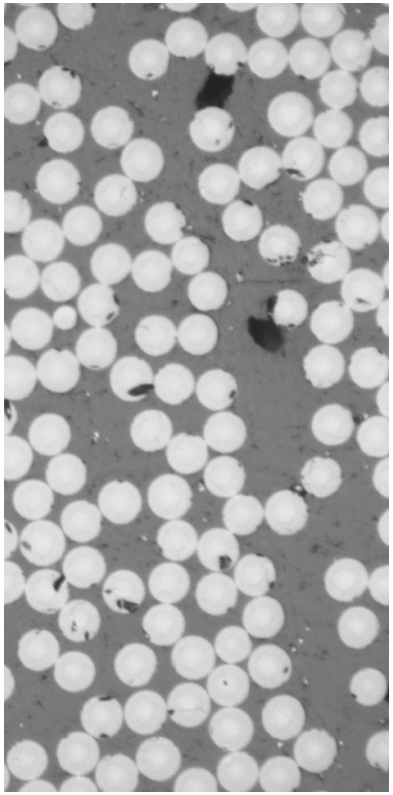

AS4/8552 UD ply cross section

Constituents:

- AS4 carbon fiber is a continuous, high strength, high strain, PAN based
- 8852 mid-toughened, high strength, damage-resistant, structural epoxy enriched with thermoplastic particles
- AS4/8552 interface

Material

AS4/8552:

- Carbon Fiber Reinforced Polymer (V_f = 58%)
- Provided by the customer (Airbus)
- UD stacking sequence is $[0]_{12}$
- Autoclave cured (2h T=130 C + 2h T=180 C at 6.2 bar)

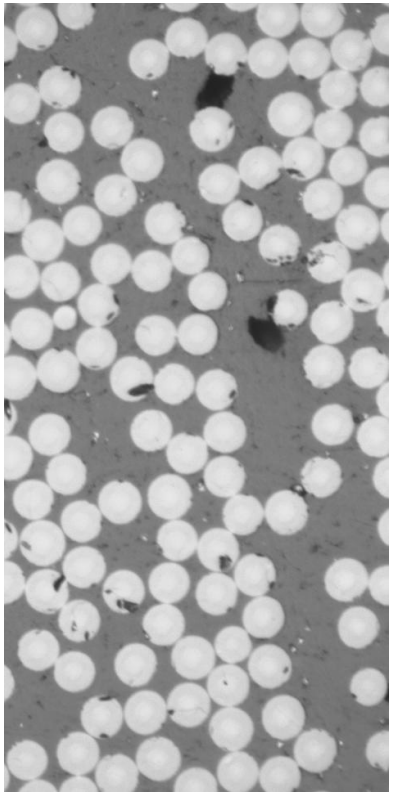

AS4/8552 UD ply cross section

Constituents:

- AS4 carbon fiber is a continuous, high strength, high strain, PAN based
- 8852 mid-toughened, high strength, damage-resistant, structural epoxy enriched with thermoplastic particles
- AS4/8552 interface

Polymer pressure dependence

Polymeric materials are largely affected by the hydrostatic pressure

Drucker-Prager $q = p \tan \beta - d$

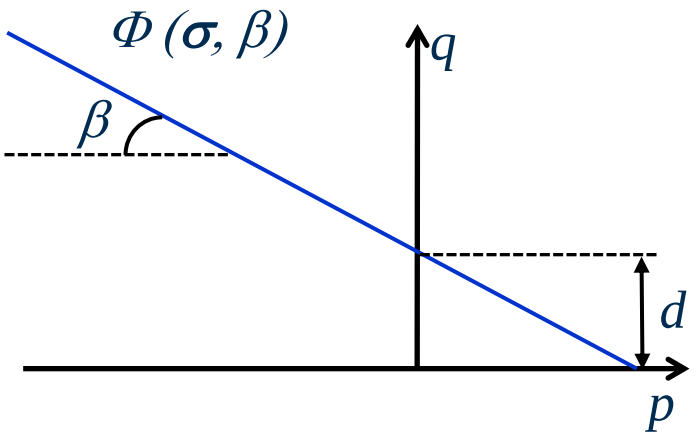

q Von Mises Equivalent Stress

p Hydrostatic Pressure Stress

β D-P Frictional Angle

d Cohesion = $f(\sigma_{yc}, \beta)$

Von Mises Material has β = 0°

Polymer can be modeled according to a modified Drucker-Prager depending on $\boldsymbol{\sigma_{yc}}$, ***E*** and **β**

Objectives of micromechanical testing

Experimental micromechanics

INSTRUMENTED NANOINDENTATION

Matrix indentation

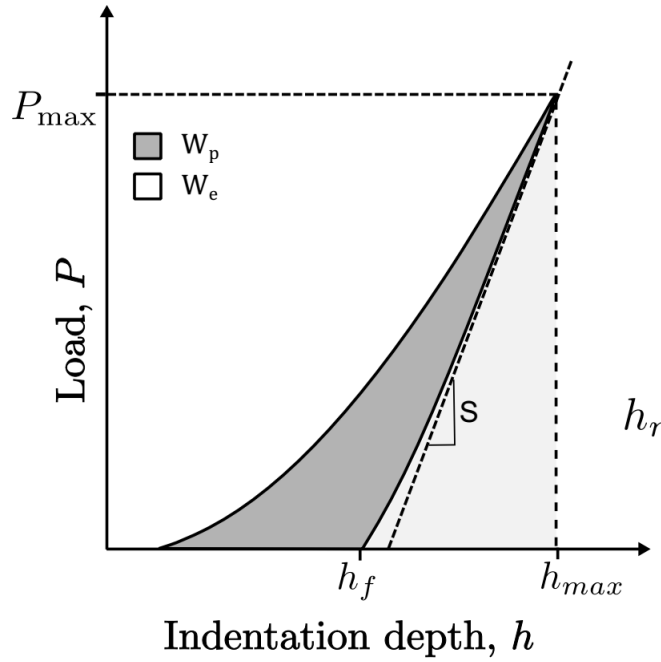

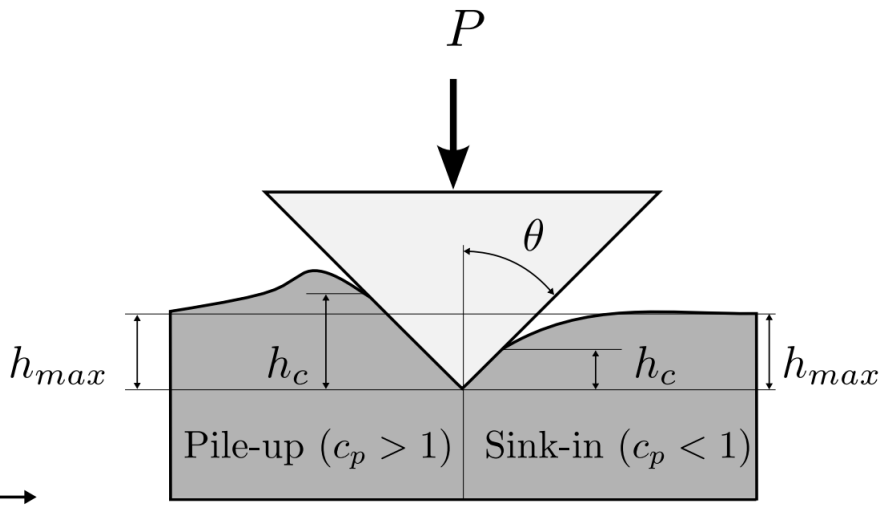

- Load (*P)* vs. indenter depth (*h)* is continuously monitored
- Contact area (A_c) determined from h_{max} and *S*, knowing the geometry of the tip (Oliver & Pharr)
- *Hardness* (H) is related to the compression strength (σ_{yc})

Matrix indentation

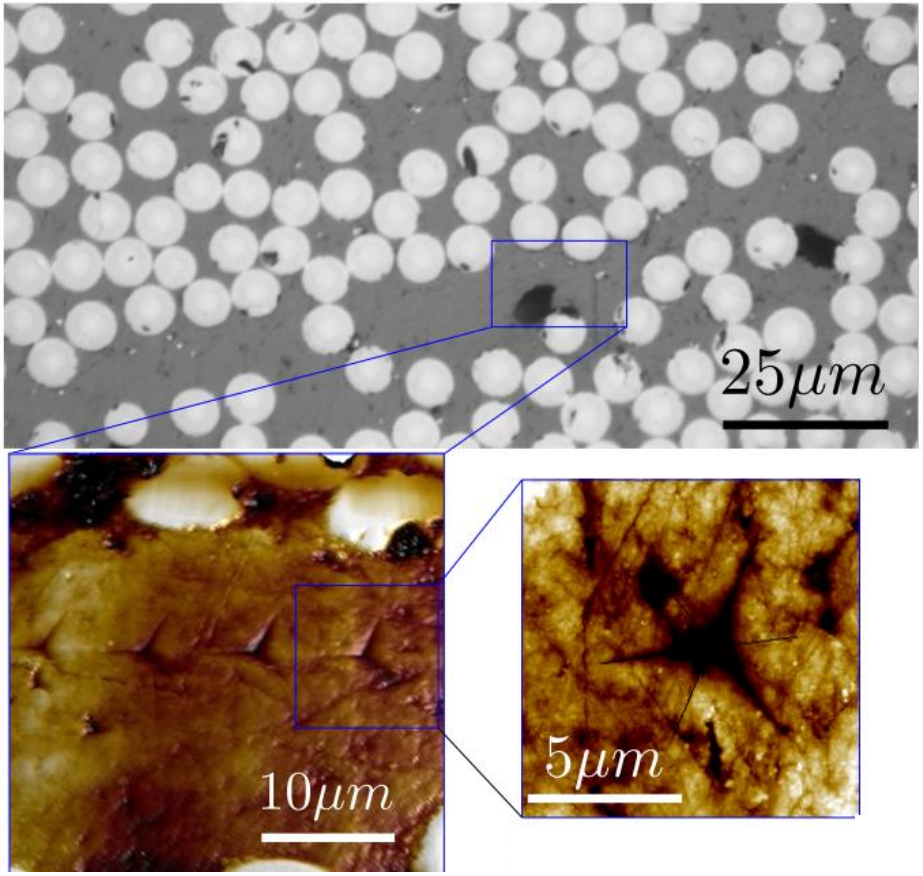

Indentations are carried out on the matrix rich regions using a **Berkovich** pyramidal indenter

Test main output: Young modulus (E), hardness (H), elastic and plastic work (W_e and W_p)

→ **Polymer pressure dependency (β)**

Matrix indentation

Master Curves as a function of H_{ap}

$$H_{ap} = \frac{P}{A_{max}}$$

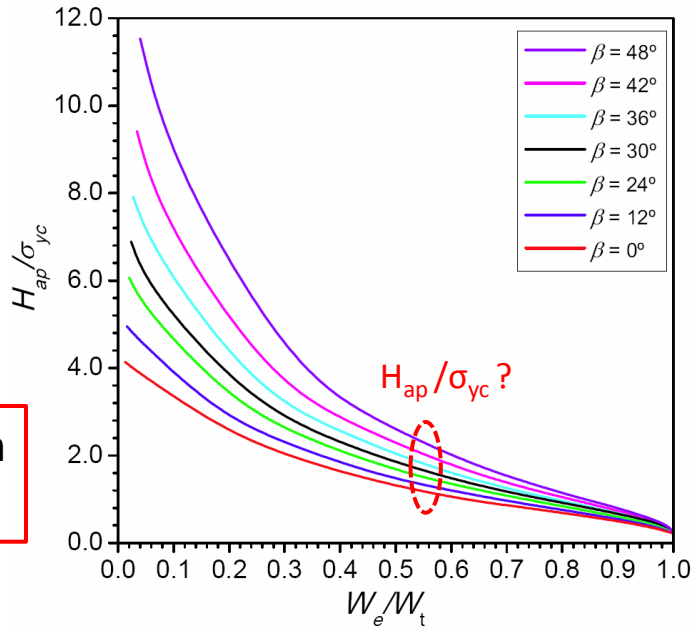

The methodology allows to determine σ_{yc} from the indentation data when β is known [2]

Condition	Hap	We/Wt	β	σyc(MPa)	E(GPa)
RT/DRY	297 ± 30	0.5477	???	???	5.07 ± 0.3

[2] Rodríguez M, Molina-Aldareguía JM, González C, LLorca J. Determination of the mechanical properties of amorphous materials through instrumented nanoindentation. Acta Mater 2012;60:3953–64.

Experimental micromechanics

MICROPILLAR COMPRESSION

Micropillar compression

Dual beam (SEM/FIB)

Nanoindenter

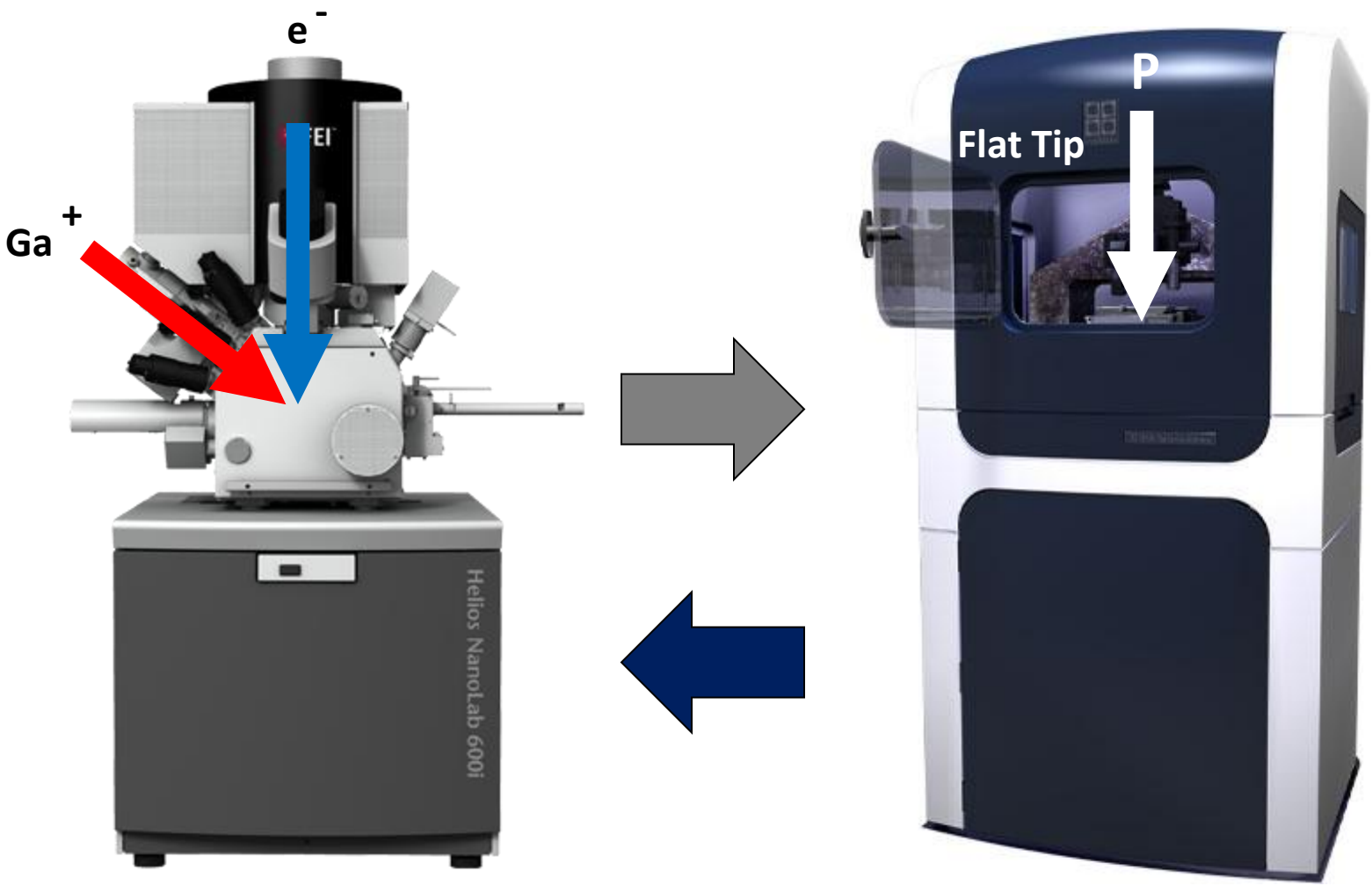

Micropillar compression

Dual beam

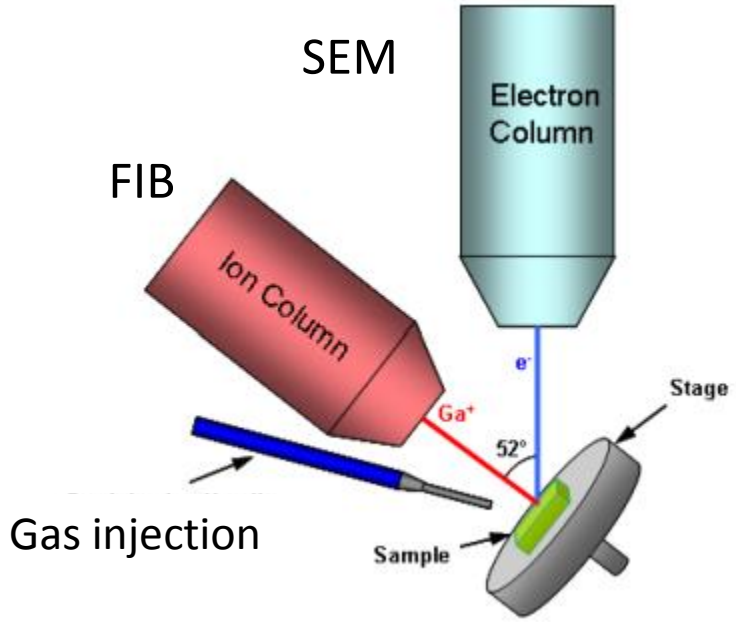

Nanoindenter

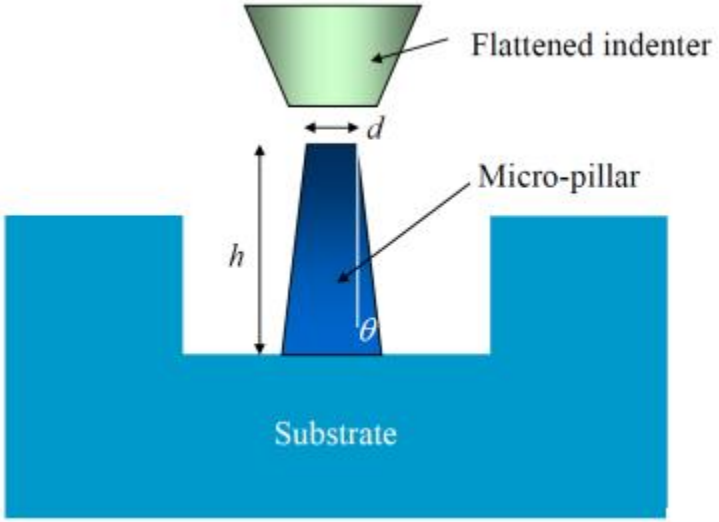


Pillar carved on the AS4/8852 resin pockets
HV
1.00 kV
curr
0.69 nA
HFW
254 µm
mag
500 x
WD
4.0 mm
det
ETD
mode
SE
tilt
30 °
z
4.0433 mm
50 µm
IMDEA Materials

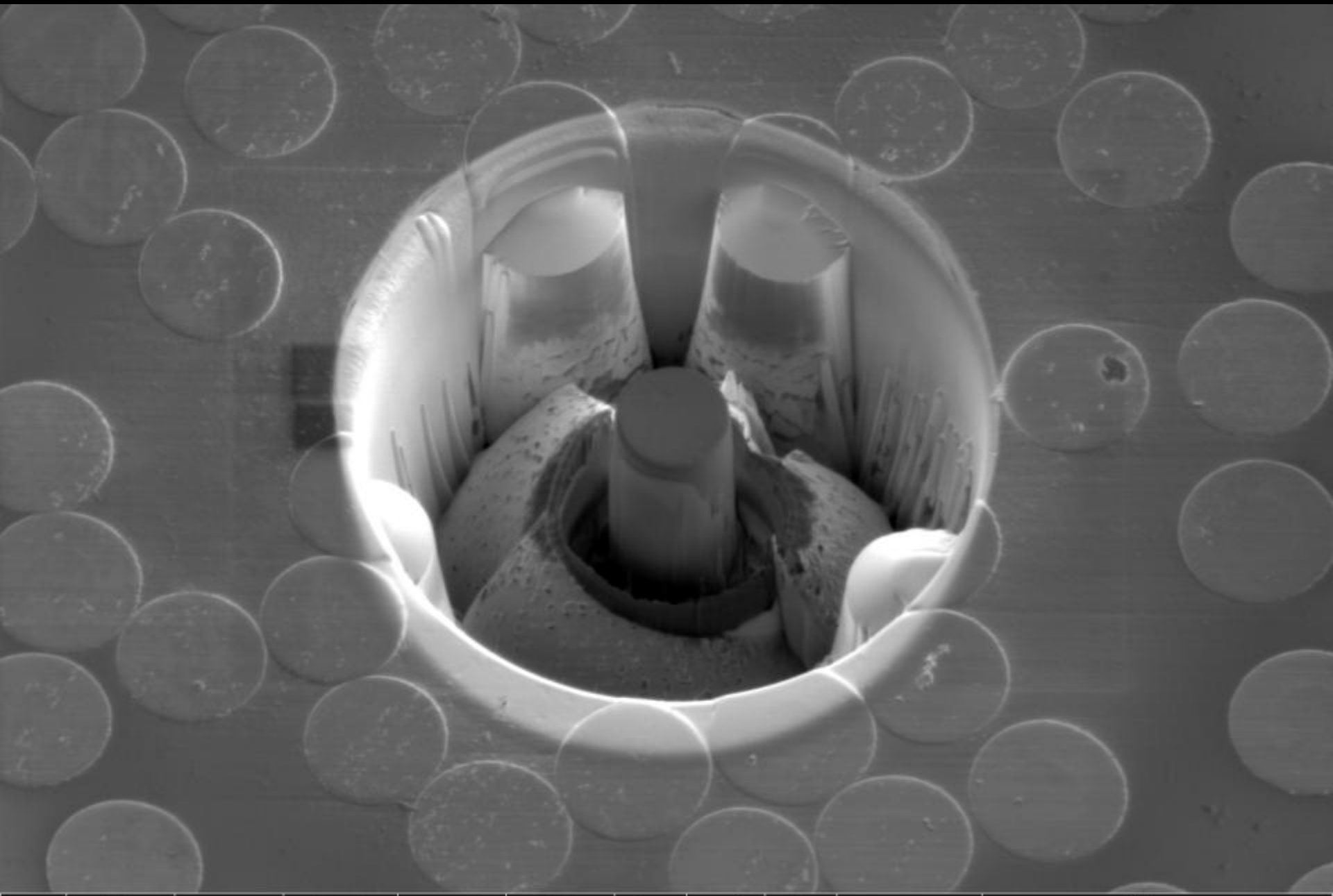
HV
1.00 kV
curr
0.69 nA
HFW
63.5 µm
mag
2 000 x
WD
4.0 mm
det
ETD
mode
SE
tilt
30 °
z
4.0430 mm
10 µm
IMDEA Materials

Micropillar compression

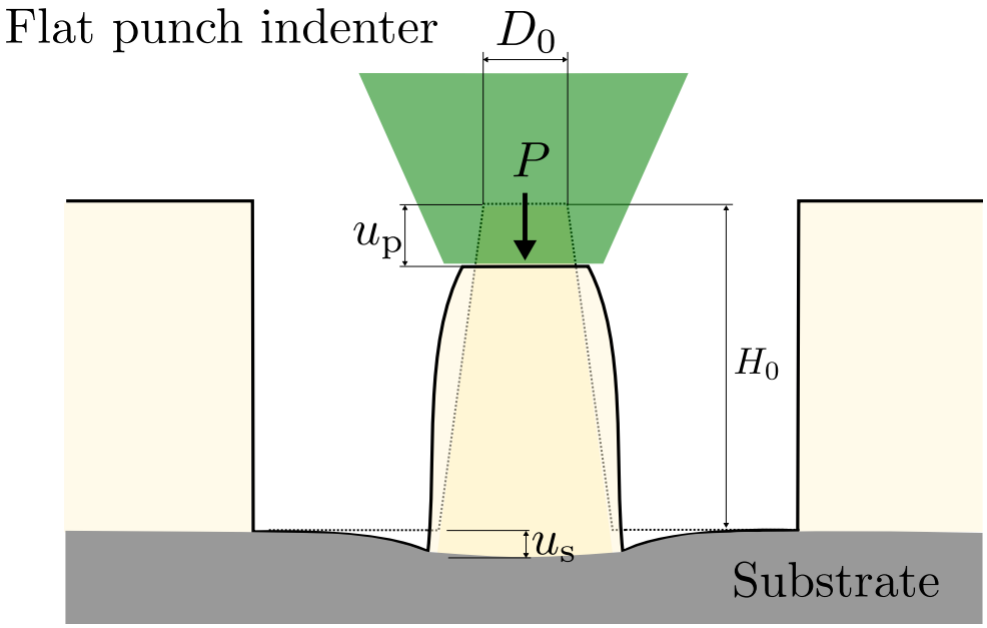

Load-displacement curve → Stress-strain curve

→Substrate and pillar are made of the same material!

→Influence of pillar geometry!

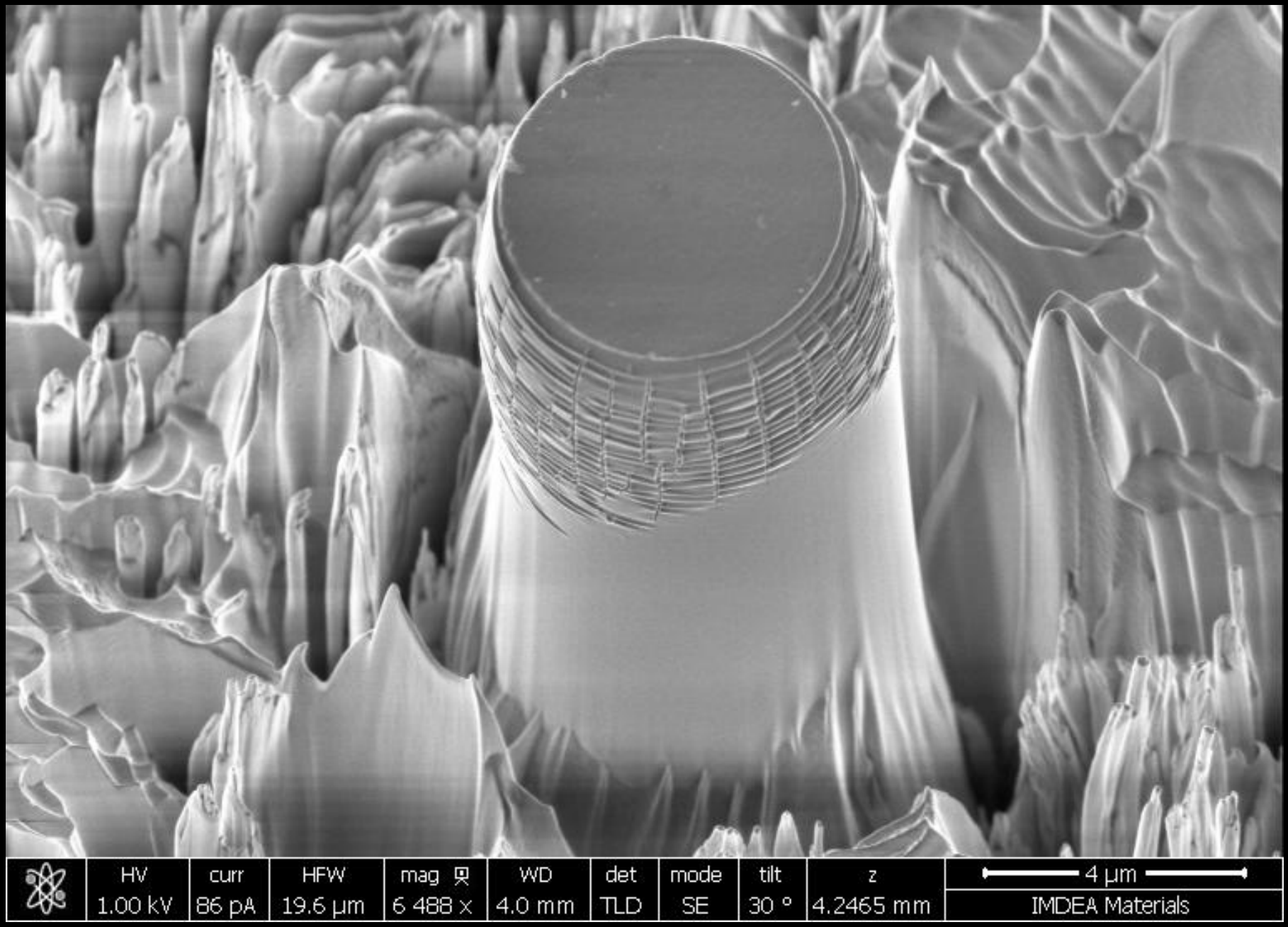

Strain concentration due to taper angle

Micropillar geometry

$$E = \Psi\left(\frac{H}{D_0}, \beta, \frac{\rho}{D_0}\right) \cdot \left(1 + \frac{\pi(1-\upsilon)D_0}{8H}\right) \cdot \frac{4H}{\pi D_0 (D_0 + 2H \cdot \tan\beta)} \cdot \frac{dP}{dh}$$

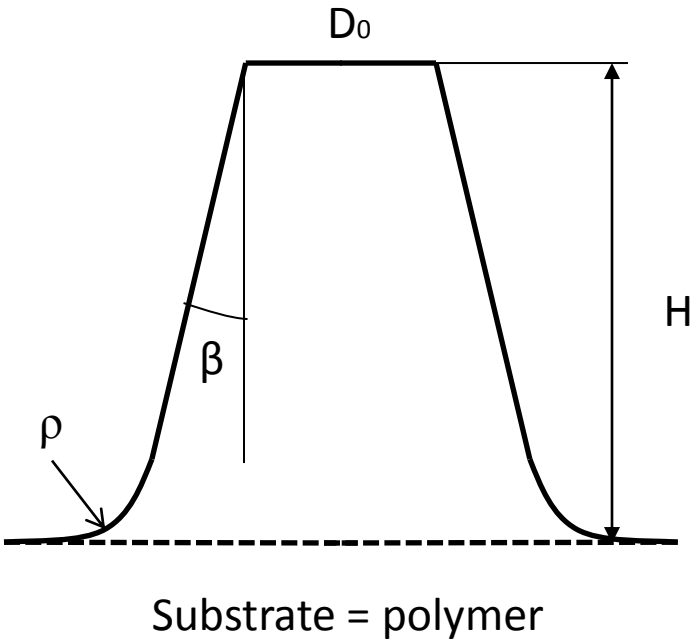

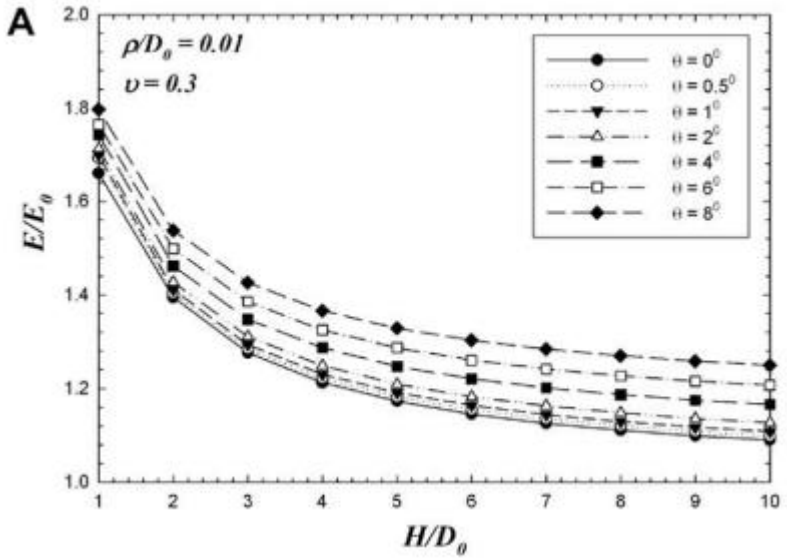

[3] Y. Yang, J.C. Ye, J. Lu, F.X. Liu, P.K. Liaw, Effects of specimen geometry and base material on the mechanical behavior of focused-ion-beam-fabricated metallic-glass micropillars, Acta Mater. 57 (2009) 1613–1623.

Micropillar compression

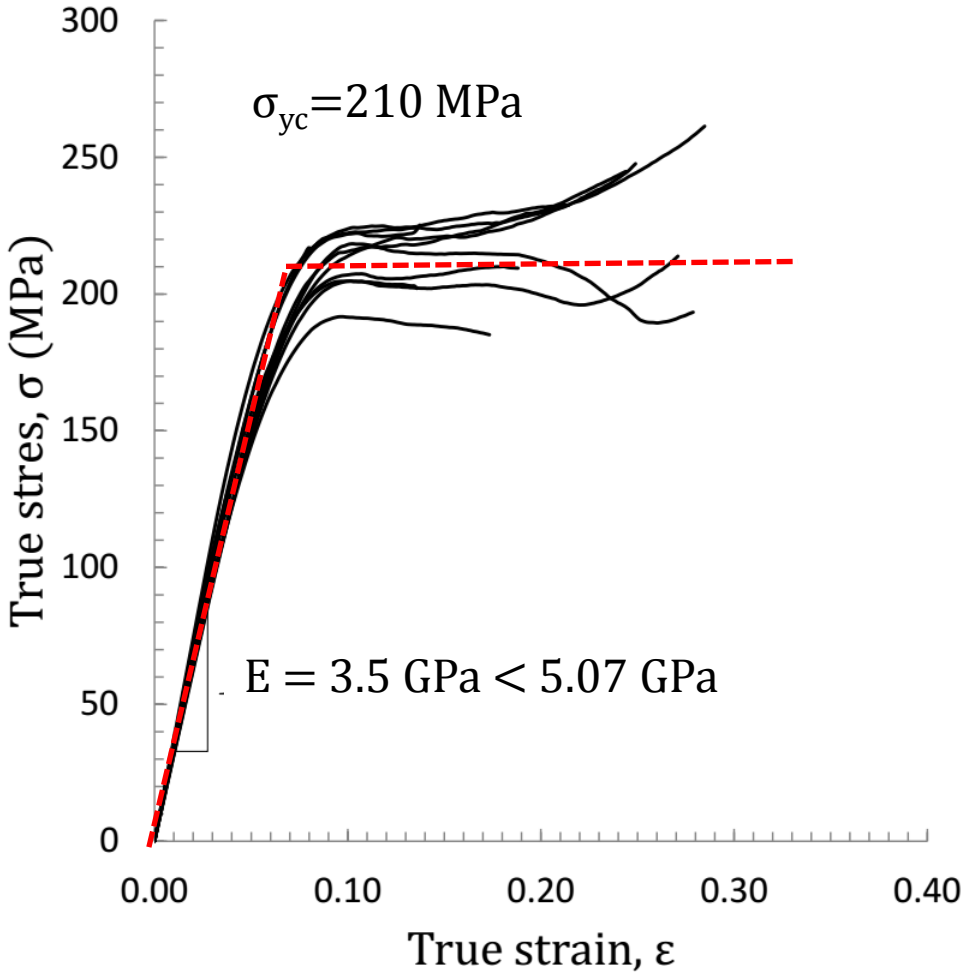

Test comparison

Test method	σ_{yc} (MPa)	E (GPa)
Nanoindentation	???	5.07
Micropillar compression	210	3.5

Young modulus provided by the supplier, E = 4.67 GPa
(tensile test ASTM D 638)

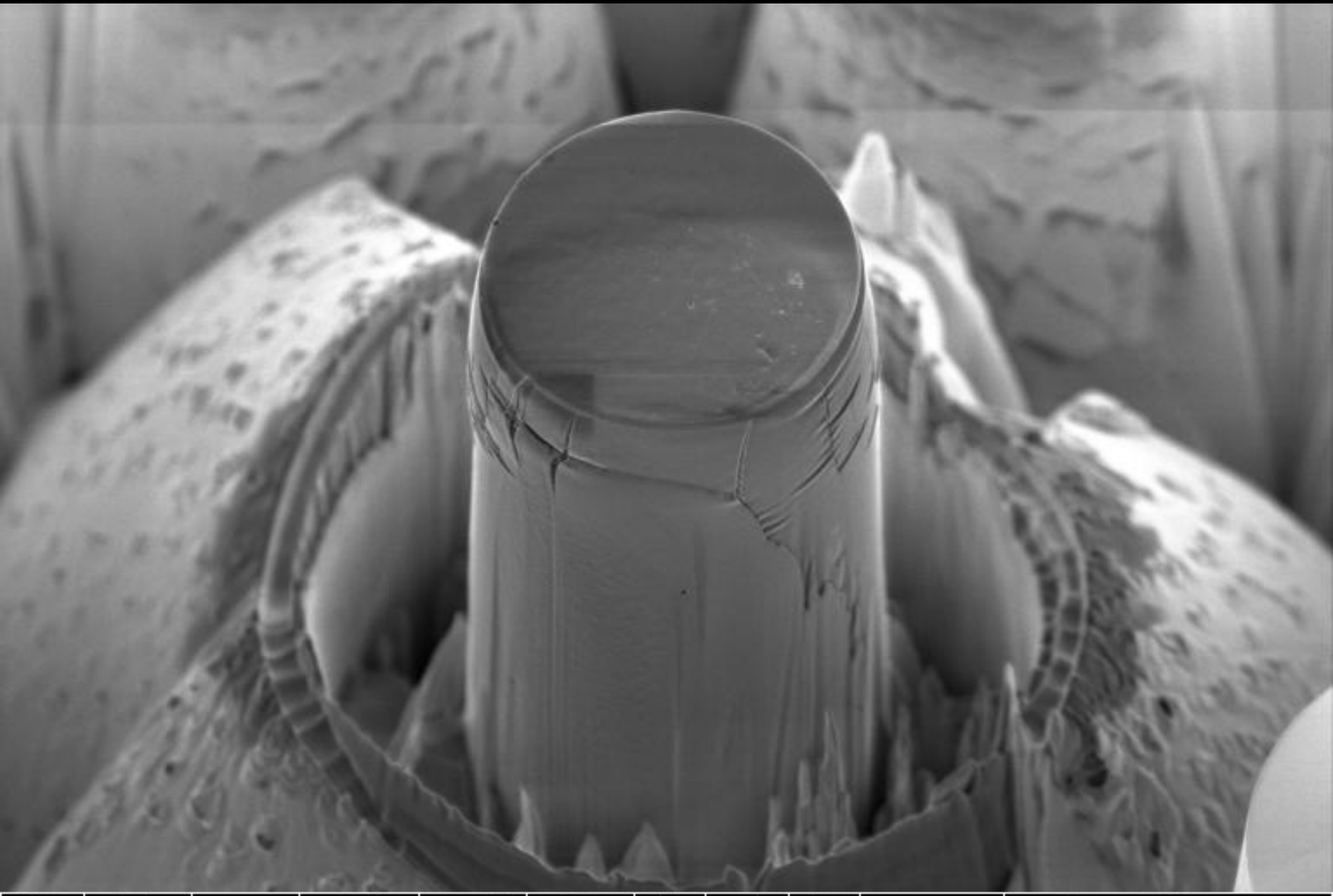
HV
1.00 kV
curr
0.17 nA
HFW
19.5 µm
mag
6 500 x
WD
4.0 mm
det
TLD
mode
SE
tilt
30 °
z
4.1756 mm
3 µm
IMDEA Materials

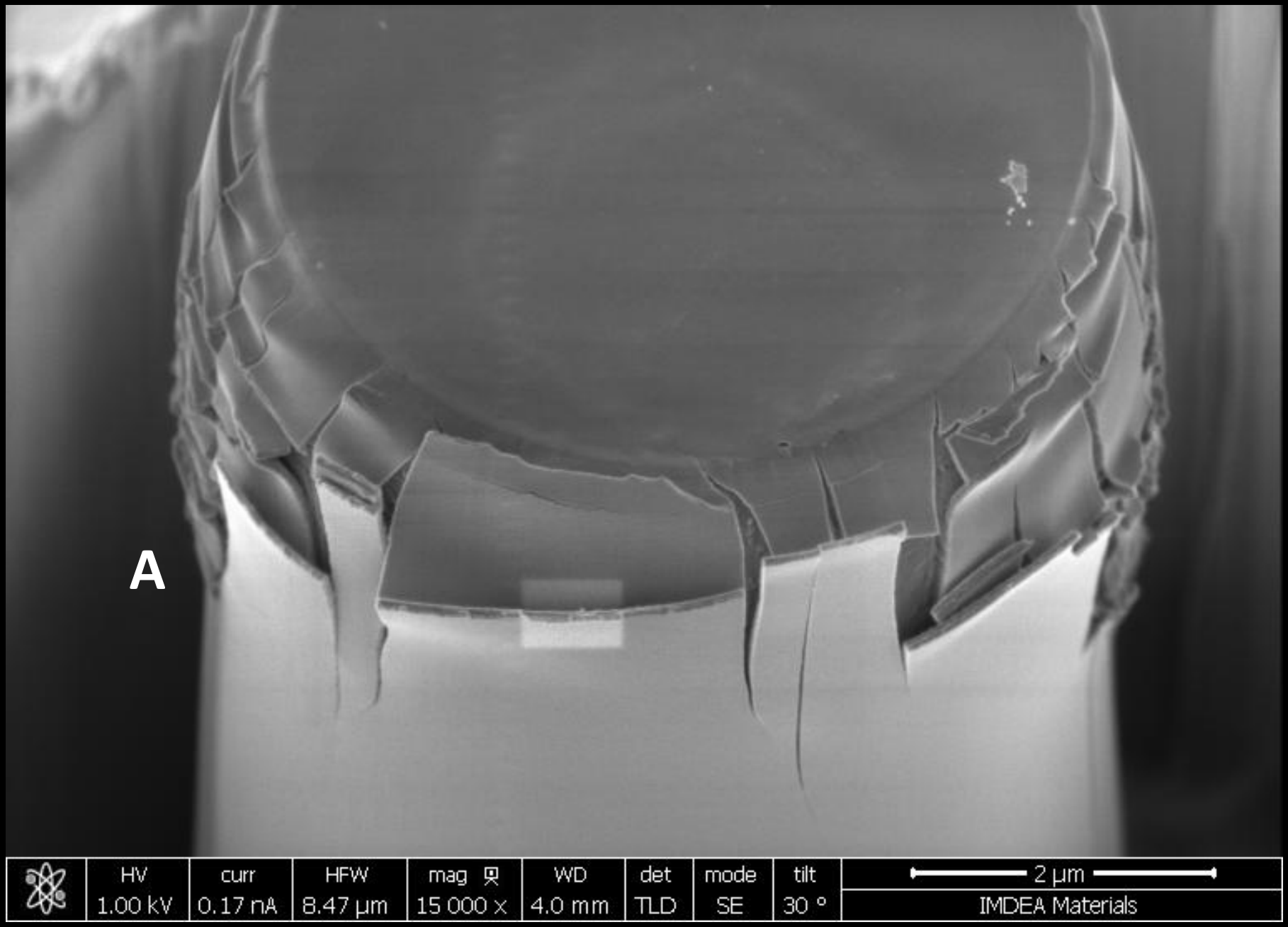

Stiff skin due to FIB attack

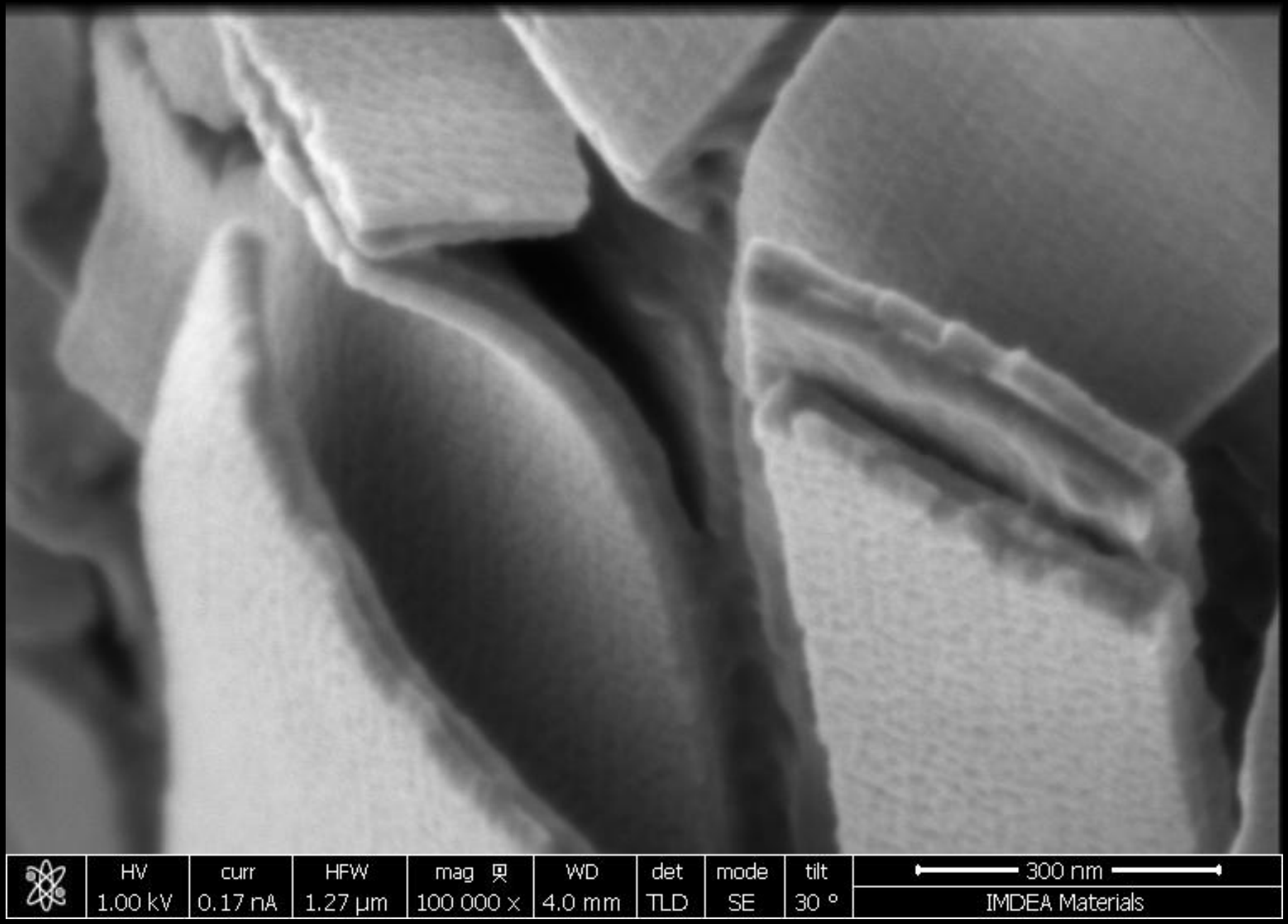

Stiff skin due to FIB attack (detail A)

Micropillar stiff skin

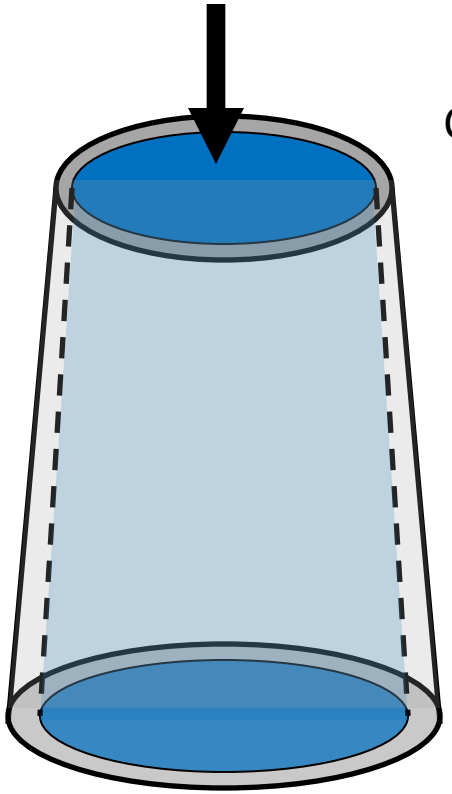

Composite material under isostrain condition

$$E_{core} = \frac{E - 4E_{skin}\left(\frac{t_{skin}}{D_0} - \left(\frac{t_{skin}}{D_0}\right)^2\right)}{\left(1 - \frac{2t_{skin}}{D_0}\right)^2}$$

$$t_{skin} = 19nm$$

$$E_{skin} = 30GPa$$

[4] S. Wang, Y. Yang, L.M. Zhou, Y.-W. Mai, Size effect in microcompression of epoxy micropillars, J. Mater. Sci. 47 (2012) 6047–6055.

Test comparison

Applying both corrections for skin and pillar geometry…

Test method	σ_{yc} (MPa)	E (GPa)
Nanoindentation	???	5.07
Micropillar compression	210 ???	~~3.5~~ 4.3

Young modulus provided by the supplier, E = 4.67 GPa
(tensile test ASTM D 638)

Now, the Young modulus derived from micropillar compression is closer to the one found by means of instrumented nanoindentation

Pillar size effect

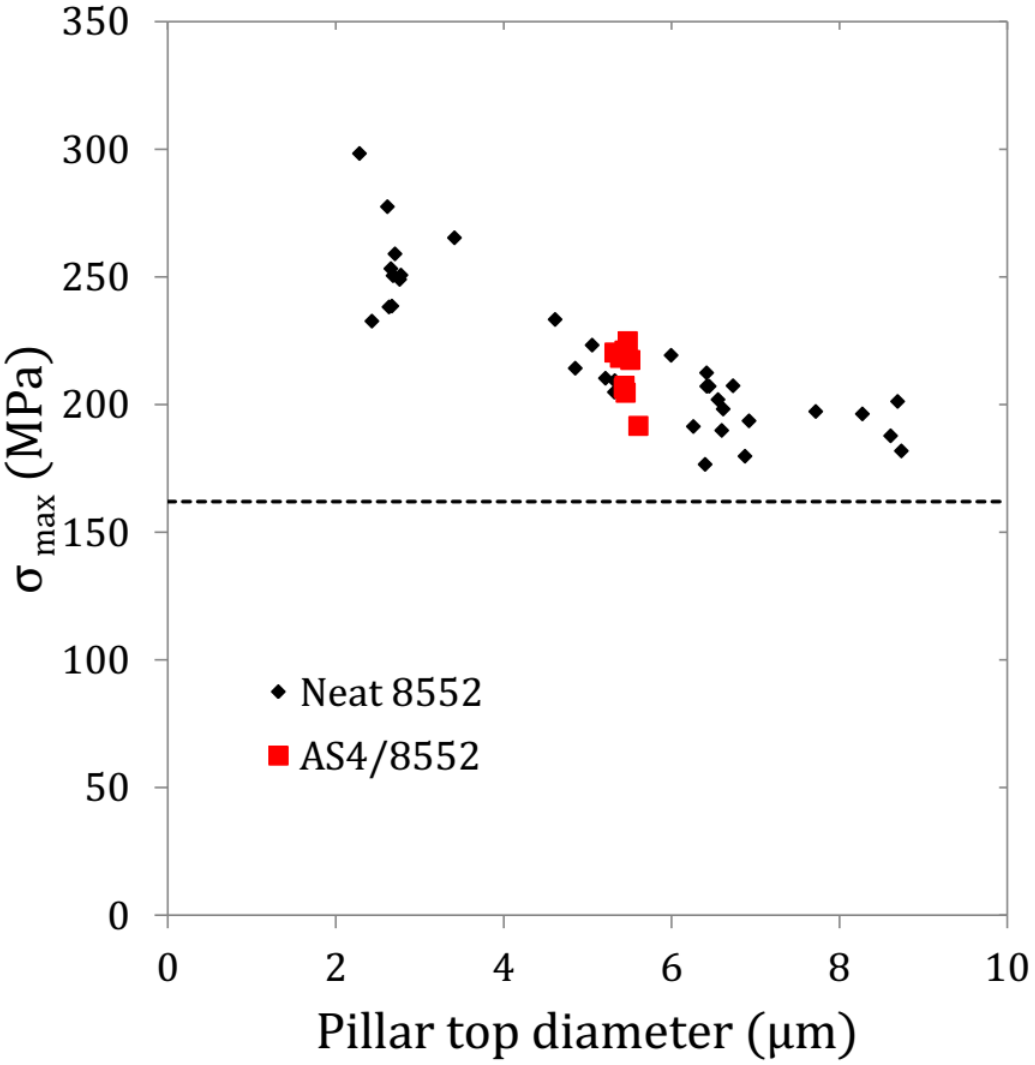

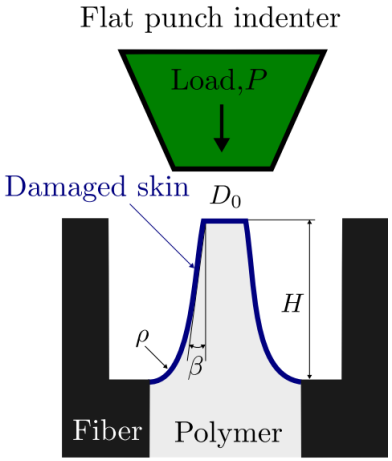

Pillar size effect

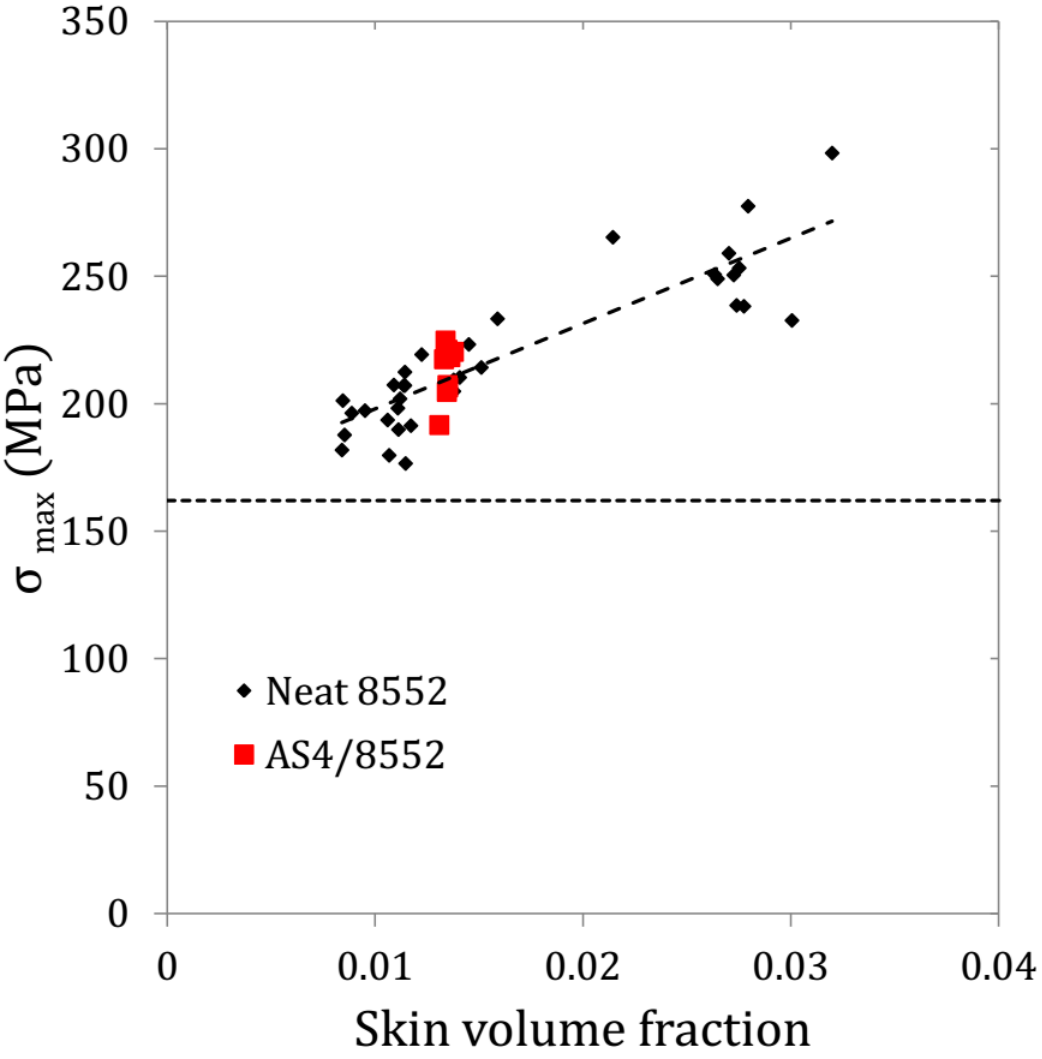

$V_{f,skin} \rightarrow 0$

$\sigma_{max} \rightarrow$ 165 MPa

Combined methodology

Applying both corrections for skin size and pillar geometry...

Test method	σ_{yc} (MPa)	E (GPa)
Nanoindentation	???	5.07
Micropillar compression	~~210~~ 165	~~3.5~~ 4.3

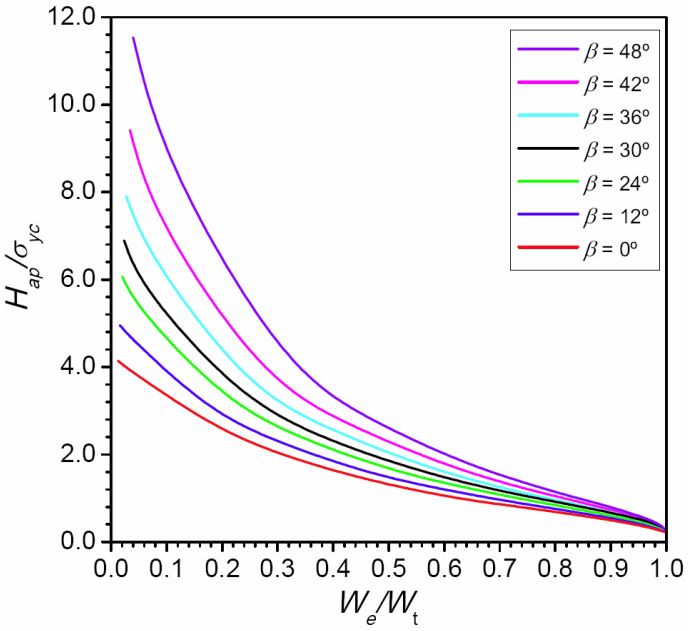

E (GPa)	σ_{yc} (MPa)	β(°)
4.3-5.07	165	30

Mater curves → β corresponding to σ_{yc} obtained from the micropillar compression tests

Conclusions & future

Conclusions

- Polymer matrix **elasto-plastic behavior** has been determined, according to a Drucker-Prager constitutive model, combining **different micromechanical experimental techniques** : instrumented nanoindentation and micropillar compression tests
- Major advantages and drawbacks of both experimental techniques when applied to polymer characterization have been pointed out
- **Micropillar compression** stands out a promising technique that can applied for **polymers characterization**. It has potential for **in-situ** application (as instrumented nanoindentation) while provides an **direct** measurement of the **stress-strain curve** (as macro compression test)

Future work

- Study the influence of the strain rate and temperature on the micropillar response
- Study the visco-elastic properties of the polymer by means of micropillar creep tests
- Explore the influence of new pillar geometries in the mechanical properties

Thank you for your attention

fernando.naya@imdea.org

miguel.monclus@imdea.org

jon.molina@imdea.org

carlosdaniel.gonzalez@imdea.org

claudiosaul.lopes@imdea.org

institute imdea materials

Instrumented indentation

Advantages

- In-situ technique (it can take into account residual thermal stresses, manufacturing and environmental conditions)
- Sample preparation and test simplicity
- Well-known technique already used at IMDEA

Disadvantages

- Interpretation can be complicated (it depends on the material type)
- It requires additional tests to estimate E, σ_{yc} and β
- Tends to overestimate material stiffness due to fiber constraint effect
- Finding resin pocket on the composite cross-section is not straightforward
- Non-conventional equipment is required

Micropillar compression

Advantages

- Stress strain curves are easy to obtain
- In-situ technique potential (micropillars can be carved anywhere on the composite cross-section)
- High resolution offering the possibility of real time monitoring of the deformation

Disadvantages

- Non-conventional equipment is required
- Stress-strain curves depend on pillar geometry (dimensions have to be determined accurately)
- FIB induced damage affects the measurements

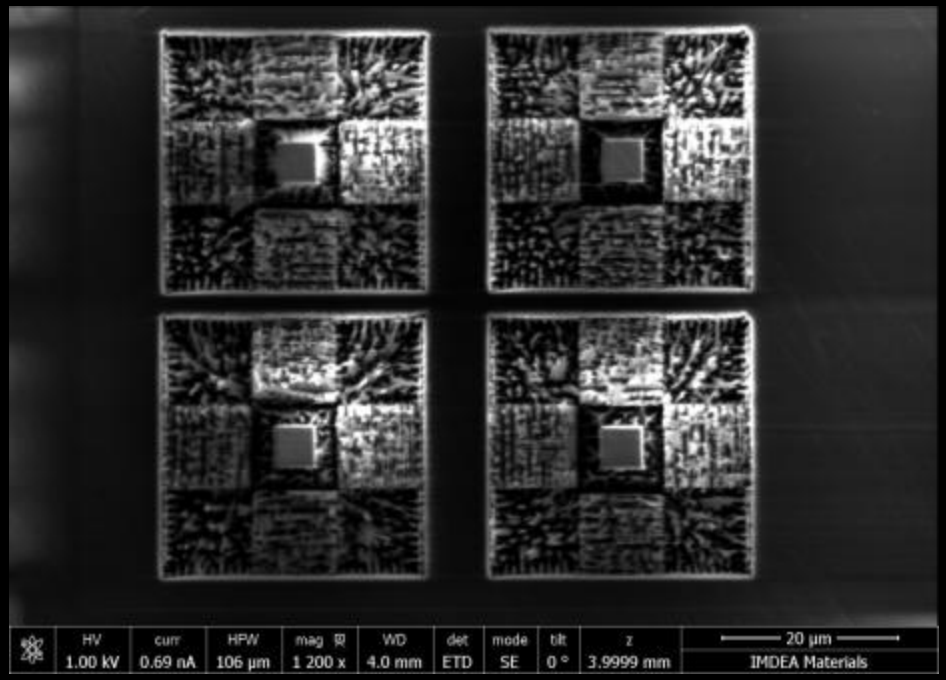
HV 1.00 kV
curr 0.69 nA
HFW 106 µm
mag 1 200 x
WD 4.0 mm
det ETD
mode SE
tilt 0 °
z 3.9999 mm
20 µm
IMDEA Materials

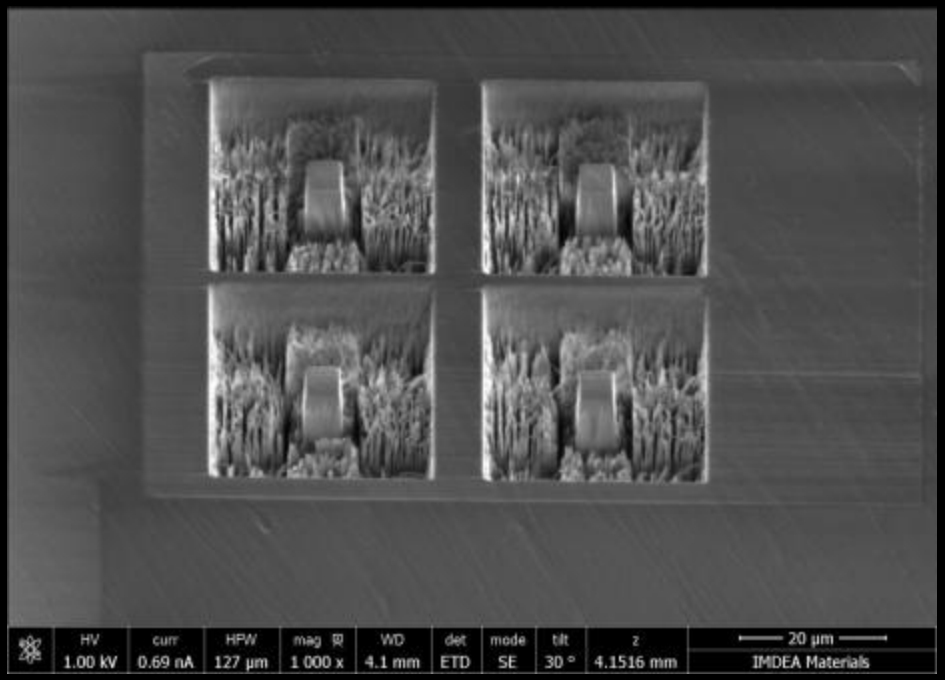
HV 1.00 kV
curr 0.69 nA
HFW 127 µm
mag 1 000 x
WD 4.1 mm
det ETD
mode SE
tilt 30 °
z 4.1516 mm
20 µm
IMDEA Materials

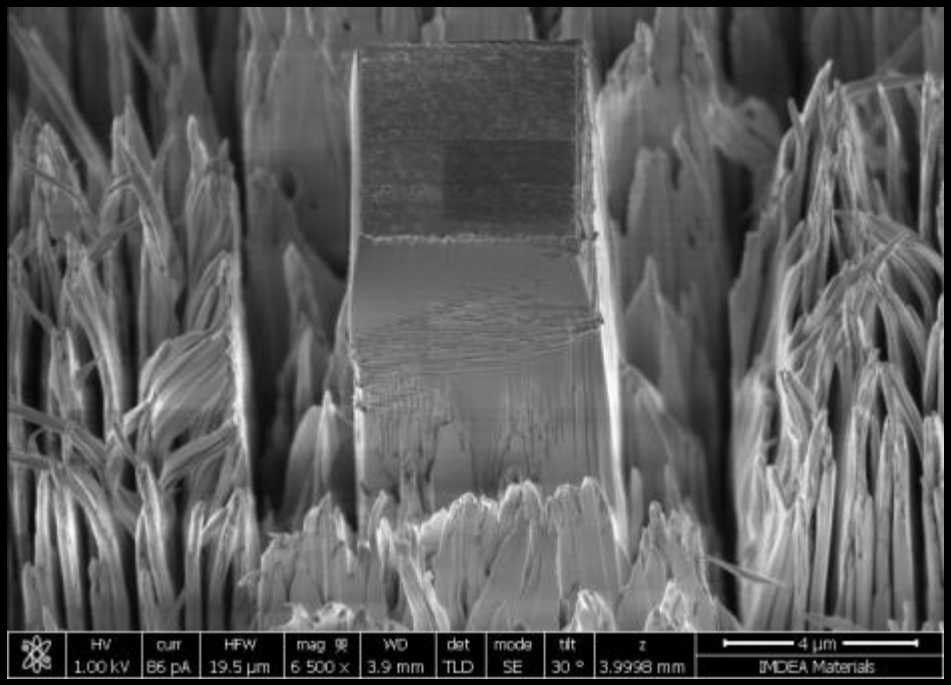
HV 1.00 kV
curr 86 pA
HFW 19.5 µm
mag 6 500 x
WD 3.9 mm
det TLD
mode SE
tilt 30 °
z 3.9998 mm
4 µm
IMDEA Materials

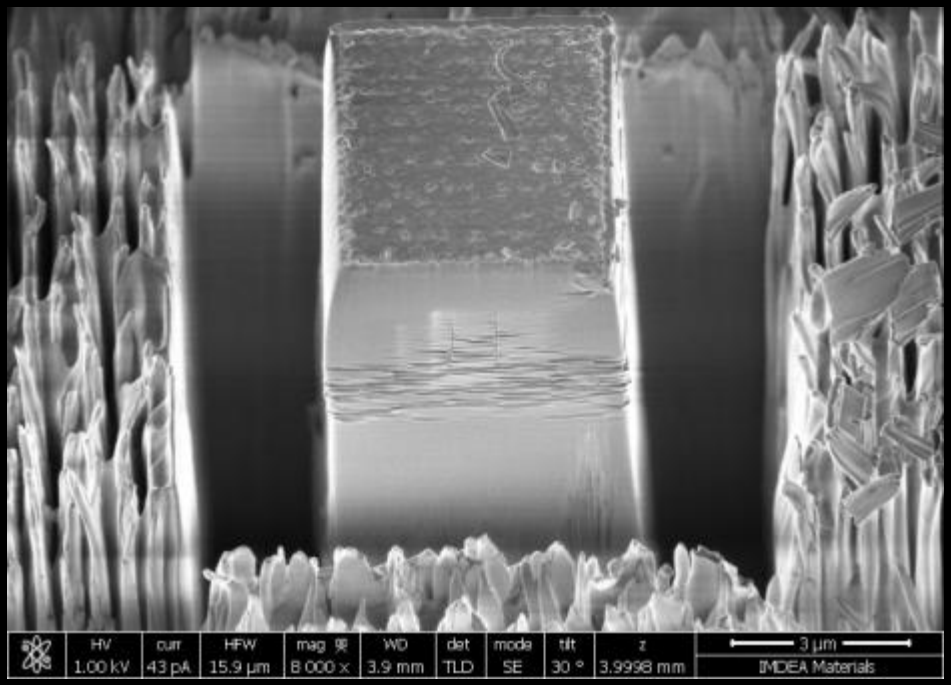
HV 1.00 kV
curr 43 pA
HFW 15.9 µm
mag 8 000 x
WD 3.9 mm
det TLD
mode SE
tilt 30 °
z 3.9998 mm
3 µm
IMDEA Materials

Macroscopic compression

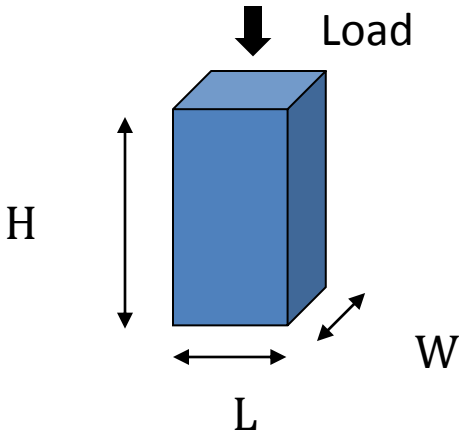

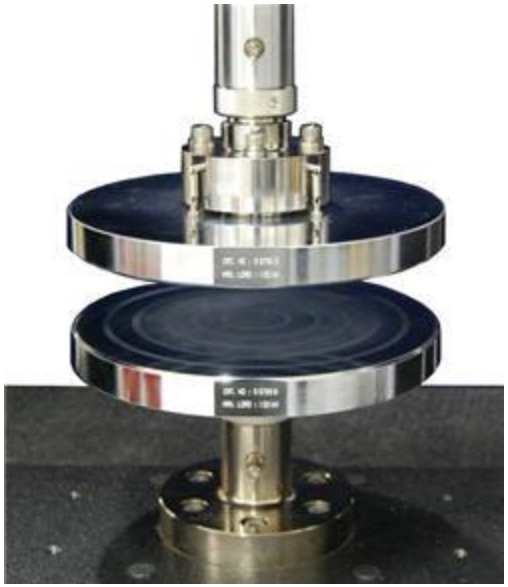

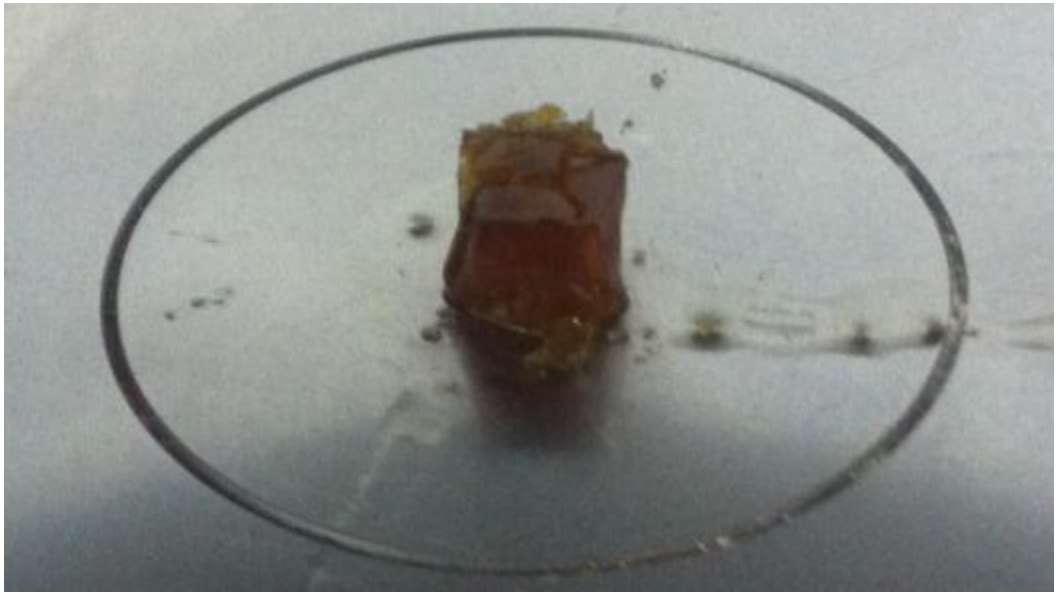

Macroscopic compression

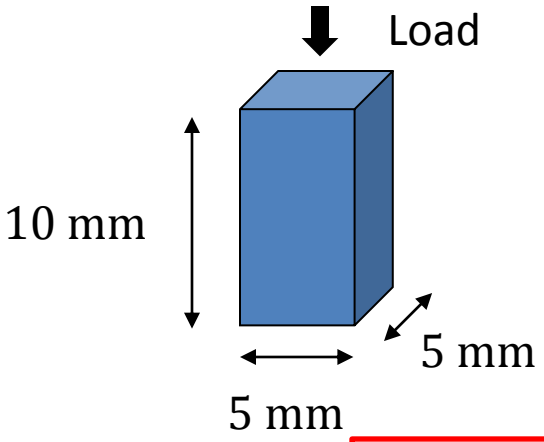

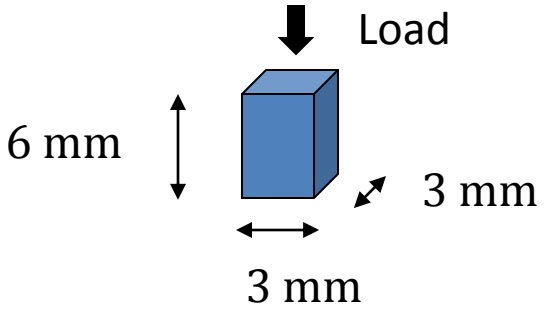

Machine compliance included